

The Trypanocidal Activity of Amidine Compounds Does Not Correlate with Their Binding Affinity to *Trypanosoma cruzi* Kinetoplast DNA[∇]

A. Daliry,¹ M. Q. Pires,² C. F. Silva,¹ R. S. Pacheco,² M. Munde,³ C. E. Stephens,³ A. Kumar,³ M. A. Ismail,³ Z. Liu,³ A. A. Farahat,³ S. Akay,³ P. Som,³ Q. Hu,³ D. W. Boykin,³ W. D. Wilson,³ S. L. De Castro,¹ and M. N. C. Soeiro^{1*}

Laboratório de Biologia Celular¹ and Laboratório de Sistemática Bioquímica,² Instituto Oswaldo Cruz, Fundação Oswaldo Cruz, Rio de Janeiro, Brazil, and Department of Chemistry, Georgia State University, Atlanta, Georgia³

Received 18 February 2011/Returned for modification 19 June 2011/Accepted 23 July 2011

Due to limited efficacy and considerable toxicity, the therapy for Chagas' disease is far from being ideal, and thus new compounds are desirable. Diamidines and related compounds such as arylimidamides have promising trypanocidal activity against *Trypanosoma cruzi*. To better understand the mechanism of action of these heterocyclic cations, we investigated the kinetoplast DNA (kDNA) binding properties and trypanocidal efficacy against *T. cruzi* of 13 compounds. Four diamidines (DB75, DB569, DB1345, and DB829), eight arylimidamides (DB766, DB749, DB889, DB709, DB613, DB1831, DB1852, and DB2002), and one guanylhydrazone (DB1080) were assayed in thermal denaturation (T_m) and circular dichroism (CD) studies using whole purified *T. cruzi* kDNA and a conserved synthetic parasite sequence. The overall CD spectra using the whole kDNA were similar to those found for the conserved sequence and were indicative of minor groove binding. Our findings showed that some of the compounds that exhibited the highest trypanocidal activities (e.g., DB766) caused low or no change in the T_m measurements. However, while some active compounds, such as DB766, induced profound alterations of kDNA topology, others, like DB1831, although effective, did not result in altered T_m and CD measurements. Our data suggest that the strong affinity of amidines with kDNA *per se* is not sufficient to generate and trigger their trypanocidal activity. Cell uptake differences and possibly distinct cellular targets need to be considered in the final evaluation of the mechanisms of action of these compounds.

Protozoan parasites display a wide range of peculiarities, including polycistronic transcription, trans-splicing of precursor mRNAs, the anchoring of surface proteins by glycosylphosphatidylinositol (GPI), and the presence of glycosomes, and this is likely due to the early divergence of the eukaryotic lineage (15). Mitochondrial DNA organization and the RNA-editing process are remarkable features of kinetoplastids, which harbor a single mitochondrion enclosing a unique type of DNA organization called kinetoplast DNA (kDNA), consisting of thousands of interlocked circular DNA molecules, referred to as minicircles and maxicircles (19). Minicircles comprise approximately 90% of the network mass, while maxicircles are present in several dozen copies (32). The major transcripts of maxicircles are mitochondrial rRNA and components of the mitochondrial oxidative phosphorylation system (32). Several maxicircle genes are modified by the RNA-editing process through uridine (U) insertions or by removal from pre-mRNA transcripts, which is catalyzed by multiprotein complexes known as editosomes (1). Editing specificity is directed by small RNAs called guide RNAs (gRNAs), which are

encoded mainly by the minicircles and are complementary to the edited sequences in maxicircle pre-mRNAs (36).

Although the kinetoplastid minicircles of most species are heterogeneous in sequence, a common feature of their nucleotide organization is the presence of conserved regions of approximately 100 to 200 bp (30). In *Crithidia fasciculata* and *Trypanosoma lewisi*, there are two copies of the conserved sequence oriented as direct repeats located 180° apart on the minicircle (29), while in *T. cruzi* there are four copies located 90° apart (12). Within these conserved sequences there is a 13-bp sequence (GGG GTT GGT GTA A) called the universal minicircle sequence (UMS) that also is present in minicircles from other trypanosomatids and is associated with the process of replication initiation (25). Within each of the four conserved sequences present in minicircles from *T. cruzi* there is an ~21-mer sequence that is perfectly repeated in homologous blocks (16). By comparing the minicircle sequences of different species of trypanosomatids, Ray found a smaller sequence (AGG GGC GTT C) conserved inside the minirepeats of eight different trypanosomatids that also could be associated with the replication of minicircles (30).

Benznidazole and nifurtimox are the only available drugs currently used for Chagas disease treatment; however, they are unsuitable, as they are often toxic, present variable efficacy, require extensive courses of therapy, and can lead to drug resistance. Therefore, new, effective, more selective and safer drugs are needed to treat diseases caused by kinetoplastids (37, 41).

* Corresponding author. Mailing address: Laboratório de Biologia, Celular, IOC, FIOCRUZ, Av. Brasil 4365, Manguinhos 21045-900, Rio de Janeiro, RJ, Brazil. Phone: 055 21 2562-1368. Fax: 055 21 2598-4577. E-mail: soeiro@ioc.fiocruz.br.

[∇] Published ahead of print on 1 August 2011.

Aromatic diamidines (ADs) and related compounds, such as arylimidamides (AIAs), are a promising group of heterocyclic compounds with remarkable activity against trypanosomatids both *in vitro* (9, 11, 26, 31, 33, 34) and *in vivo* (3, 22, 7). Many representatives of this class of compounds, including furamidine (DB75), accumulate in DNA-containing organelles, such as nuclei and, most notably, mitochondria (5, 18, 21, 7). Transmission electron microscopy studies showed that amidines are able to induce kDNA network disruption, fragmentation, and disappearance (5, 10, 33). Furthermore, some of them induce alterations in the mitochondrial membrane potential (9, 31, 7) and exhibit characteristics of the cationic uncoupler of oxidative phosphorylation (24). However, the exact mechanism of action of this class of compounds still is poorly understood.

Thus, in the present work our aims were (i) to evaluate the trypanocidal activity of 13 structurally related amidines and (ii) to explore their interaction with the actual parasite kDNA by the techniques of thermal denaturation (T_m) and circular dichroism (CD) using both whole purified *T. cruzi* kDNA and a conserved synthetic parasite sequence. The study is unique in its use of kDNA with the amidines and analogs (Table 1) and allowed the comparative analysis of the profile of kDNA binding affinities of the compounds with their chemical structure and trypanocidal activity.

MATERIALS AND METHODS

Parasites. Epimastigotes of the Y strain of *T. cruzi* were grown in liver infusion tryptose (LIT) medium supplemented with 10% fetal calf serum with weekly passages (4). Bloodstream trypomastigotes (BT) from the Y strain were harvested by heart puncture of infected Swiss mice at the peak of parasitemia (13).

Compounds. The synthesis of compounds was performed according to our previously reported methodology (Table 1). Stock solutions were prepared in dimethyl sulfoxide (DMSO), with the final concentration of the solvent never exceeding 0.6%. This concentration was not toxic to the parasite or mammalian host cells (data not shown). Benznidazole (2-nitroimidazole; Laboratório Farmacêutico do Estado de Pernambuco [LAFEPE], Brazil) was used as a reference drug.

***In vitro* antitrypanosomal activity.** Epimastigotes at the exponential phase of growth (5-day-old culture forms) were harvested, washed with phosphate-buffered saline (PBS), and resuspended in LIT medium at a concentration of 5×10^6 parasites/ml. The parasites then were incubated for 24 h at 28°C in the presence of increasing doses of each compound (0 to 1,000 mM) or benznidazole (0 to 250 mM) (3). After quantification using a Neubauer chamber, the IC50s (the compound concentration that reduces the number of parasites by 50%) were averaged from at least three determinations obtained in duplicate.

kDNA preparation. The methodology used for kDNA extraction was performed as previously reported by Morel et al. (23) with minor modifications (27, 35). Briefly, epimastigotes harvested during the exponential phase of growth were washed three times with centrifugation in cold SE buffer (0.15 M NaCl, 0.1 M EDTA, pH 8.0) and resuspended at a concentration of 2.5×10^8 cell/ml in SE. The lysis was performed by the addition of 0.5 mg/ml of proteinase K and 3% (wt/vol) Sarkosyl, followed by an incubation for 3 h at 60°C. The lysate then was passed through a number 18 needle six times and centrifuged for 1 h at 4°C using an SW55 rotor (L-100XP Optima ultracentrifuge; Beckman Coulter, Fullerton, CA) at 33,000 rpm. The supernatant was discarded, and the pellet was resuspended in 5 ml of TE buffer (10 mM Tris-HCl, 0.1 M EDTA, pH 7.4) and centrifuged as before. The supernatant fluid was discarded, and the kDNA pellet was resuspended in 200 ml of TE, followed by the addition of RNase (4 mg/10⁹ cells). After incubating for 1 h at 37°C, the DNA solution was extracted twice with chloroform-isoamyl alcohol (24:1) and centrifuged for 7 min at 13,000 rpm at room temperature. The aqueous phase was transferred to a clean tube, and 1 ml of ether was added. After vigorous shaking, the upper phase was discarded, and the procedure was repeated twice. The material was left to dry at room temperature, and the DNA was precipitated at -20°C overnight with 0.2 M NaCl and 3 volumes of absolute ethanol. The isolated kDNA was pelleted for 30 min

at 13,000 rpm and resuspended in TE. DNA quantification was performed by reading the absorbance at 260 nm using a spectrophotometer (GeneQuant Pro RNA/DNA calculator; GE Healthcare Life Sciences, Cambridge, England).

Restriction endonuclease treatment. Purified kDNA was digested with three different enzymes: EcoRI, HindIII, and HinfI (Promega, Madison, WI). The reaction was performed in a total volume of 30 ml containing 1× enzyme buffer, 2 U of each enzyme, and 1 mg of DNA. The mixture was incubated for 3 h at 37°C, and 15 ml (0.5 mg) was used for gel electrophoresis.

PCR. For the PCR amplification, 0.2 µg of purified kDNA was used in a total reaction volume of 25 ml containing 1× PCR buffer, 0.2 mM minicircle-specific primers of our design (5' TGG ATG GTT TTG GGA GGG GCG 3' and 3' CCA ACC CCA ATC GAA CCC CAC C 5'), 1.5 mM MgCl₂, 200 pmol dNTPs, and 0.5 U *Taq* polymerase. The samples were heated to 94°C for 2 min, followed by 35 cycles of 94°C for 15 s, 60.5°C for 30 s, and 72°C for 40 s. A final extension at 72°C was carried out for 7 min. Finally, 10 ml of each PCR product was subjected to gel electrophoresis.

Gel electrophoresis. Agarose gels (0.8%) in 1× TBE buffer (89 mM Tris base, 89 mM boric acid, and 2 mM EDTA, pH 8.3) were used. Gels were stained with either ethidium bromide (0.5 mg/ml) for 1 h or SYBR Gold nucleic acid gel stain at the concentration and time recommended by the manufacturer (Invitrogen, Carlsbad, CA).

Conserved sequence of *T. cruzi* minicircles. The conserved sequence used in the CD and T_m experiments was designed based on the minicircle nucleotide sequences reported for Y strain (accession number M18814) available in the GenBank database (www.ncbi.nlm.nih.gov/GenBank), and it was synthesized by Integrated DNA Technologies (IDT; Atlanta, GA) using 5' GTT TTG GGA GGG GCG TTC AAA T 3' and 3' CAA AAC CCT CCC CGC AAG TTT A 5'.

Thermal melting analysis. The thermal melting experiments were conducted as previously reported (2, 21). The ΔT_m values were determined by following the absorption change at 260 nm as a function of temperature and were calculated using the following equation: $\Delta T_m = T_{mc} - T_{mf}$, where T_{mc} is the melting temperature of the complex compound DNA and T_{mf} is the melting temperature of the free nucleic acid.

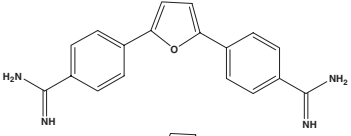
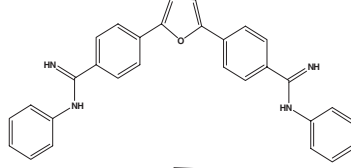
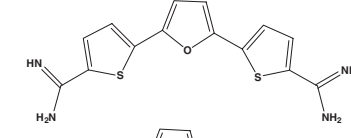
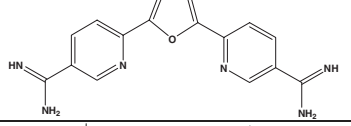
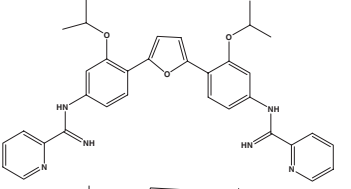
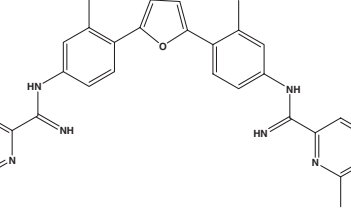
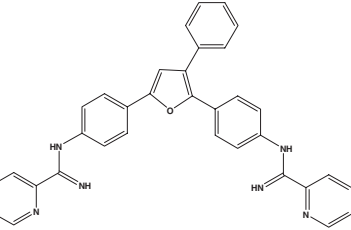
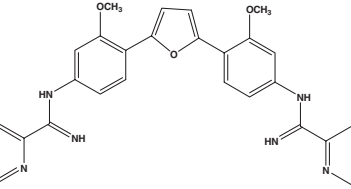
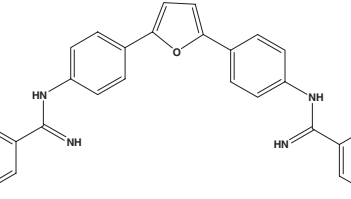
The T_m values were determined from the first derivative plots. Experiments were done with 15×10^{-6} M DNA in 10 mM cacodylic acid buffer (pH 6.25) and 0.01 mM NaCl in 1-cm quartz cuvettes in a 0.2 ratio (compound:DNA) using a Cary 300 Bio spectrophotometer (Agilent Technologies, Santa Clara, CA) with the software supplied with the instrument.

CD. CD analyses were performed as previously described, with minor modifications (2). The CD spectra were obtained using a Jasco J-810 spectrophotometer (Jasco Analytical Instruments, Easton, MD) at a scan speed of 50 nm/min. The DNA samples were scanned from 220 to 500 nm in 1-cm quartz cuvettes in a buffer consisting of 10 mM cacodylic acid buffer (pH 6.25) and 0.01 mM NaCl at 25°C. For the whole purified kDNA, a 0.2 ratio (compound:DNA) with a 15×10^{-6} M concentration of DNA was used. For the conserved synthetic sequence, aliquots of the compounds in concentrated stock solutions were titrated into the DNA at ratios indicated in the figures using the same DNA concentration mentioned above (Fig. 1A to H). The software supplied by Jasco provided instrument control and data acquisition (2). The data shown in Fig. 1 and 3 are representative of experiments that have been conducted at least three times and processed with KaleidaGraph software.

Fluorescence microscopy of kDNA. The spreading and analysis of the *T. cruzi* kDNA network was performed by fluorescent monitoring using the methodology previously reported, with minor modifications (37). Briefly, 1 mg of isolated kDNA was mixed with 1% bovine serum albumin and spread on a clean glass slide. The samples were fixed for 5 min in cold methanol, dried at room temperature, and stained with 5 mg/ml of 4',6-diamidino-2-phenylindole (DAPI). Subsequently, the samples were mounted with 2.5% 1,4-diazabicyclo[2.2.2]octane (DABCO) and analyzed with a Zeiss photomicroscope equipped with epifluorescence (Carl Zeiss Inc., Thornwood, NY). Image J software (version 1.44; National Institutes of Health, Bethesda, MD [<http://rsbweb.nih.gov/ij/>]) was used for the network area calculations using measurements for at least 50 parasites in three different biological sample analyses.

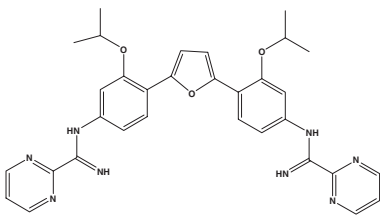
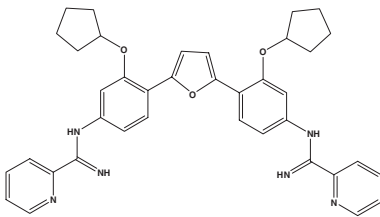
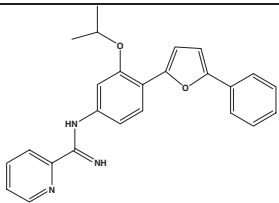
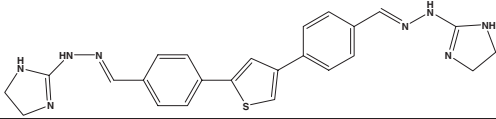
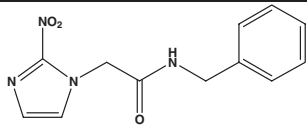
Atomic force microscopy (AFM). kDNA preparations (0.1 mg/ml) were resuspended in the following buffer: 40 mM HEPES-Cl and 10 mM MgCl₂, pH 8.0. The solution then was spread on freshly cleaved mica and allowed to stand for 5 min at 25°C. It then was rinsed with deionized water (0.2 to 0.5 ml), air-dried, and scanned on a Multimode V microscope (Veeco Instruments Inc., Plainview, NY). Nanoscope software (version 6.13; Veeco Instruments Inc., Plainview, NY) was used for the calculation of minicircle circumferences.

TABLE 1. Anti-*T. cruzi* activity (IC₅₀/24 h) against bloodstream trypomastigotes of Y strain

Compound class	Compound name	Chemical structure	IC ₅₀ /24h (μM)	Reference
Diamidines	DB75		32	(6)
	DB569		2	(7)
	DB1345		0.9	(24)
	DB829		437	(14)
Di-AIA	DB766		0.06	(43)
	DB749		1.8	(38)
	DB889		0.09	(33)
	DB709		0.09	(38)
	DB613		4	(38)

Continued on following page

TABLE 1—Continued

			0.02	NR
Di-AIA	DB1852		0.06	NR
Mono-AIA	DB2002		20.4	NR
Guanylhyazone	DB1080		0.24	(24)
Nitroheterocyclic	Bz		12.94	

^a NR, synthesis not reported. The compounds were prepared by the approaches outlined in Stephens et al. (38).

^b Bz, benzimidazole.

RESULTS

In vitro biological activity. Aiming to determine if the biological activities of amidines could be correlated with their kDNA binding properties, four ADs (DB75, DB569, DB1345, and DB829), eight AIAs (DB766, DB749, DB889, DB709, DB613, DB1831, DB1852, and DB2002), and one guanylhyazone (DB1080) were selected based on previous *in vitro* studies performed with bloodstream trypomastigotes (BT) (Table 1). However, due to the great difficulty in purifying large amounts of kDNA from the BT, experiments were conducted using epimastigotes, and then the effect of the amidines was assayed against these parasite forms. All compounds presented a dose-dependent trypanocidal activity against epimastigotes (data not shown), with IC₅₀s ranging from 0.08 to 938 mM (Table 2). Interestingly, with the exception of DB766 and DB2002, epimastigotes were less susceptible than BT to all amidines regardless of their class. For example, DB1080 was approximately 800 times less effective on epimastigotes than BT. Similar data also were found when benzimidazole was employed, reaching IC₅₀s of 12.94 and 168 mM for BT and epimastigotes, respectively (Tables 1 and 2). As observed

with BT, the most active compounds were the AIAs, especially DB766, with an IC₅₀ of 0.08 mM, which is similar to that of BT (Tables 1 and 2).

Thermodynamic studies performed with minicircles conserved sequences. The relative binding affinities of synthetic and natural compounds for nucleic acid sequences may be estimated from changes in T_m values on DNA-drug complex formation (44). We thus assessed the T_m values of different amidines for a selected synthetic conserved 22-mer sequence from Y strain of *T. cruzi* minicircles, using a compound-to-kDNA base pair ratio of 0.2 (Table 2). DB75 and DB569 showed ΔT_m of 17 and 8°C, respectively (Table 2), even though they presented low and moderate activity. Except for DB613, the AIAs (DB766, DB709, DB1831, and DB1852) showed little or no change in T_m measurements (ΔT_m ranging from 0 to 2°C) (Table 2), suggesting that although very active, they are weak binders under these tested conditions. The mono-AIA (DB2002) also presented low binding affinity to the minicircle sequence (ΔT_m of 0°C) (Table 1).

To further explore the effect of the compounds on DNA topology, their CD spectra were analyzed using the conserved

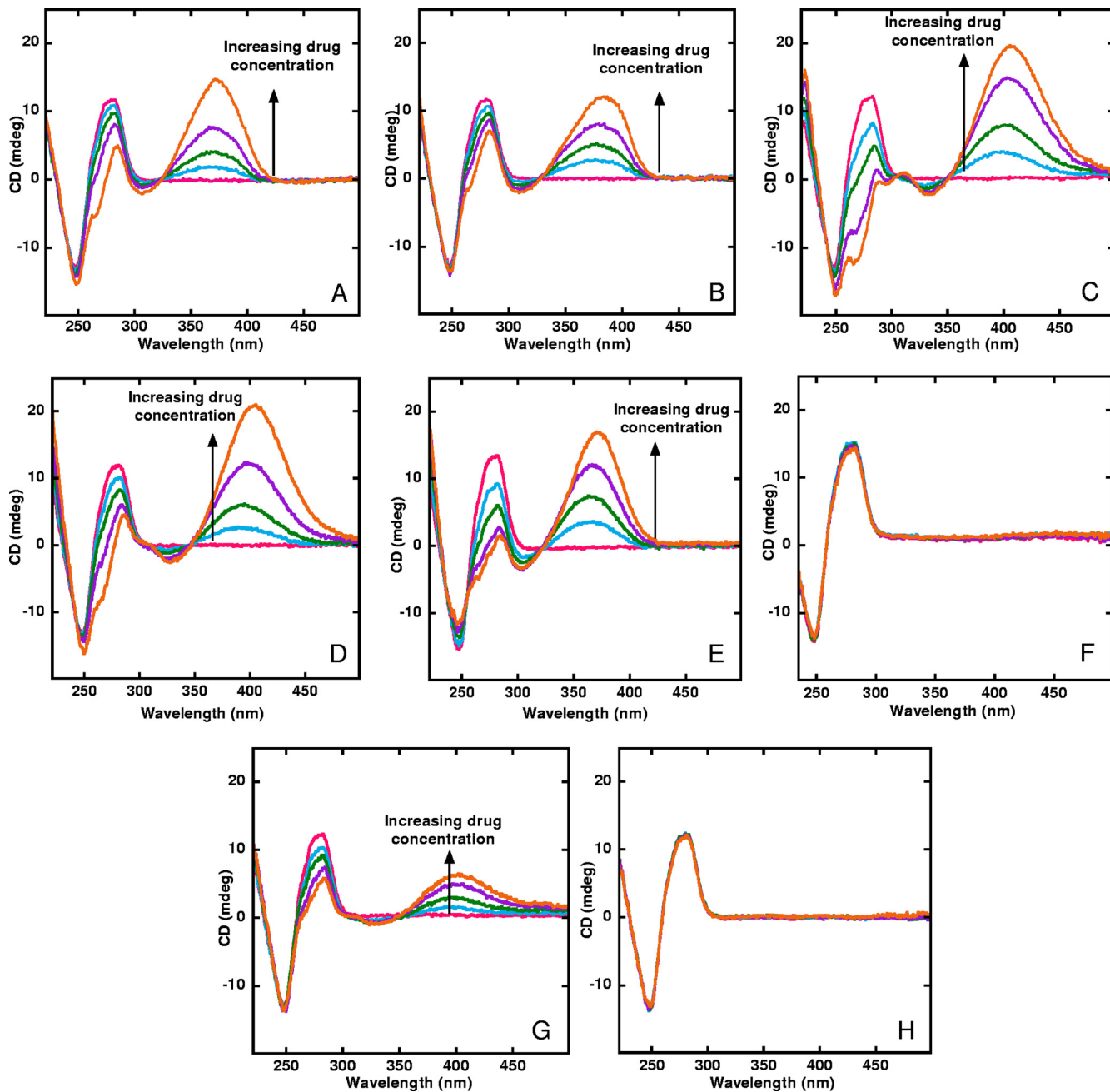


FIG. 1. (A to H) CD spectrum titration of different concentrations of each indicated amidine compound with the kDNA conserved sequence (see Materials and Methods for details). A spectrum for DNA without compound is shown in red and has no induced signal. (A) DB75; (B) DB569; (C) DB766; (D) DB709; (E) DB613; (F) DB1831; (G) DB1852; and (H) DB2002.

synthetic sequence using different ratios of compound to base pairs (0.5, 1, 2, and 4) and monitoring from 220 to 500 nm (Fig. 1A to H). Positive ratio-dependent CD signals were observed for DB75, DB569, B766, DB709, DB613, and DB1852 (Fig. 1A, B, C, D, E, and G, respectively), which are characteristic of minor groove DNA binding. In contrast, DB1831 (Fig. 1F) and DB2002 (Fig. 1H), two AIAs that have a high and a moderated effect against *T. cruzi*, respectively, induced no significant signals, suggesting a weak binding to the minicircle sequence. All compounds that showed positive induced CD also exhibited

changes of the spectra in the DNA region (260 nm) that could be attributable to compound-DNA ratio-dependent alterations in the DNA conformation (Fig. 1A, B, C, D, E, and G). None of the compounds reached saturation, even when using the highest compound-to-DNA ratio (Fig. 1A to H).

Thermodynamic studies performed with intact kDNA. As some of the most active compounds do not strongly bind to the conserved sequence, we evaluated if they could associate with other sequences present in intact whole kDNA, also using T_m and CD assays (Fig. 2 and 3 and Table 2). Before performing the T_m

TABLE 2. Anti-*T. cruzi* activity ($IC_{50}/24$ h) upon Y strain of epimastigote forms and relative DNA binding affinities (ΔT_m) of amidines to minicircle conserved sequence and kDNA-purified network^a

Compound	IC_{50} (μM)	ΔT_m ($^{\circ}C$)	
		Conserved sequence	kDNA network
Diamidines			
DB75	790 \pm 296	17 \pm 2	15 \pm 1
DB569	7.2 \pm 2	8 \pm 1	15 \pm 1
DB1345	725 \pm 120	ND	14 \pm 0
DB829	938 \pm 25	ND	9 \pm 1
Di-AIA			
DB766	0.08 \pm 0.02	1 \pm 1	3 \pm 1
DB749	15 \pm 3	ND	8 \pm 0
DB889	0.5 \pm 0.3	ND	5 \pm 1
DB709	0.8 \pm 0.5	2 \pm 2	8 \pm 0
DB613	22 \pm 6	12 \pm 0	14 \pm 0
DB1831	0.6 \pm 0.09	0 \pm 1	0 \pm 0
DB1852	2.3 \pm 1	0 \pm 0	2 \pm 2
Mono-AIA			
DB2002	11 \pm 3	0 \pm 0	0 \pm 0
Guanyldiazotone			
DB1080	207 \pm 33	ND	17 \pm 1
Nitroheterocyclic			
Bz	168 \pm 67	ND	ND

^a ND, not done; Bz, benznidazole. IC_{50} and ΔT_m are shown as means (μM and $^{\circ}C$, respectively) \pm standard deviations from at least three independent experiments each performed in duplicate.

and CD assays, the purity and integrity of the networks were verified by the amplification of specific minicircle sequences, by restriction endonuclease patterns, by fluorescence microscopy, and by AFM analyses (Fig. 2A to C). For PCR amplification, specific primers (see Materials and Methods) that amplify a 230-bp fragment present in the kDNA of *T. cruzi* were designed

based on the minicircle sequence with accession number M18814 in the GenBank database (<http://www.ncbi.nlm.nih.gov/GenBank>). After PCR, a band of the expected size (230 bp) was amplified and visualized in an agarose gel (data not shown), providing the first indication of the presence of minicircles in the purified fraction. The incubation of the isolated kDNA fractions with different restriction endonuclease enzymes (HindIII, EcoRI, and HinfI) resulted in a consistent pattern of restriction fragments characteristic of *T. cruzi* kDNA (Fig. 2A) (23, 28). Through fluorescence microscopy (Fig. 2B) and AFM analyses (Fig. 2C), the integrity of the kDNA networks purified from epimastigotes was further assessed. DAPI staining of intact parasites allows the identification of the nuclei and the kDNA (Fig. 2B, inset). When the isolated kDNA was adhered to glass slides and stained with DAPI, round fluorescent networks were observed (Fig. 2B), with network areas ranging between 20 and 39 μm^2 (data not shown). AFM images captured by tapping mode revealed a kDNA network composed of minicircles consisting of small interconnected circles with sizes of $\sim 0.5 \mu m$ (Fig. 2C). We also observed the presence of larger circles that were $\sim 1 \mu m$ in size. These assays confirmed that the methodology employed for the kDNA purification was suitable for the next steps of the study.

The T_m data determined using intact *T. cruzi* kDNA demonstrated that except for DB709 and DB569, the incubation of whole kDNA with the compounds resulted in similar binding patterns (Table 2), as previously shown with the synthetic conserved sequences. In the case of DB569 and DB709, we observed a significantly higher binding affinity for the whole kDNA (ΔT_m of 15 and 8 $^{\circ}C$, respectively), which suggests that it could be targeting sequences other than the conserved sequence used (Table 2).

The overall CD spectra of the whole kDNA also were similar to those found for the conserved sequences, showing a minor groove binding ability and changes in the DNA region (Fig. 3A to M). In the assays using native kDNA, usually ADs and AIAs presented different changes in the spectra in the DNA range, with AIAs exhibiting greater induced conformational changes (Fig. 3E to I).

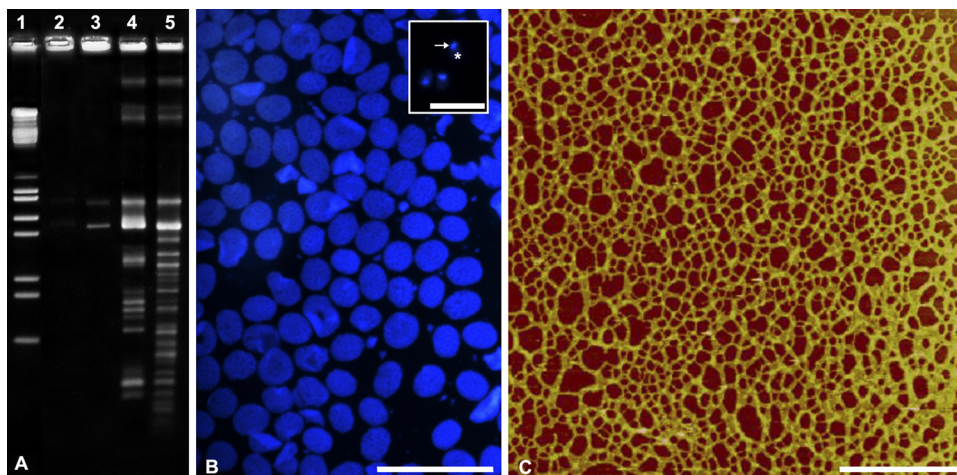


FIG. 2. (A) Agarose gel (0.8%) of isolated kDNA from epimastigote forms of *T. cruzi* subjected to restriction endonucleases. Lane 1, EcoRI/HindIII molecular marker; lane 2, untreated kDNA; lane 3, kDNA treated with HindIII; lane 4, kDNA treated with EcoRI; lane 5, kDNA treated with HinfI. (B) Fluorescence microscopy image of the purified kDNA network stained with DAPI. The inset shows live epimastigotes stained with DAPI; the arrow indicates the kDNA, and asterisks indicate the nuclei. Bar = 20 μm . (C) AFM micrograph of the kDNA-purified network. Bar = 2 μm .

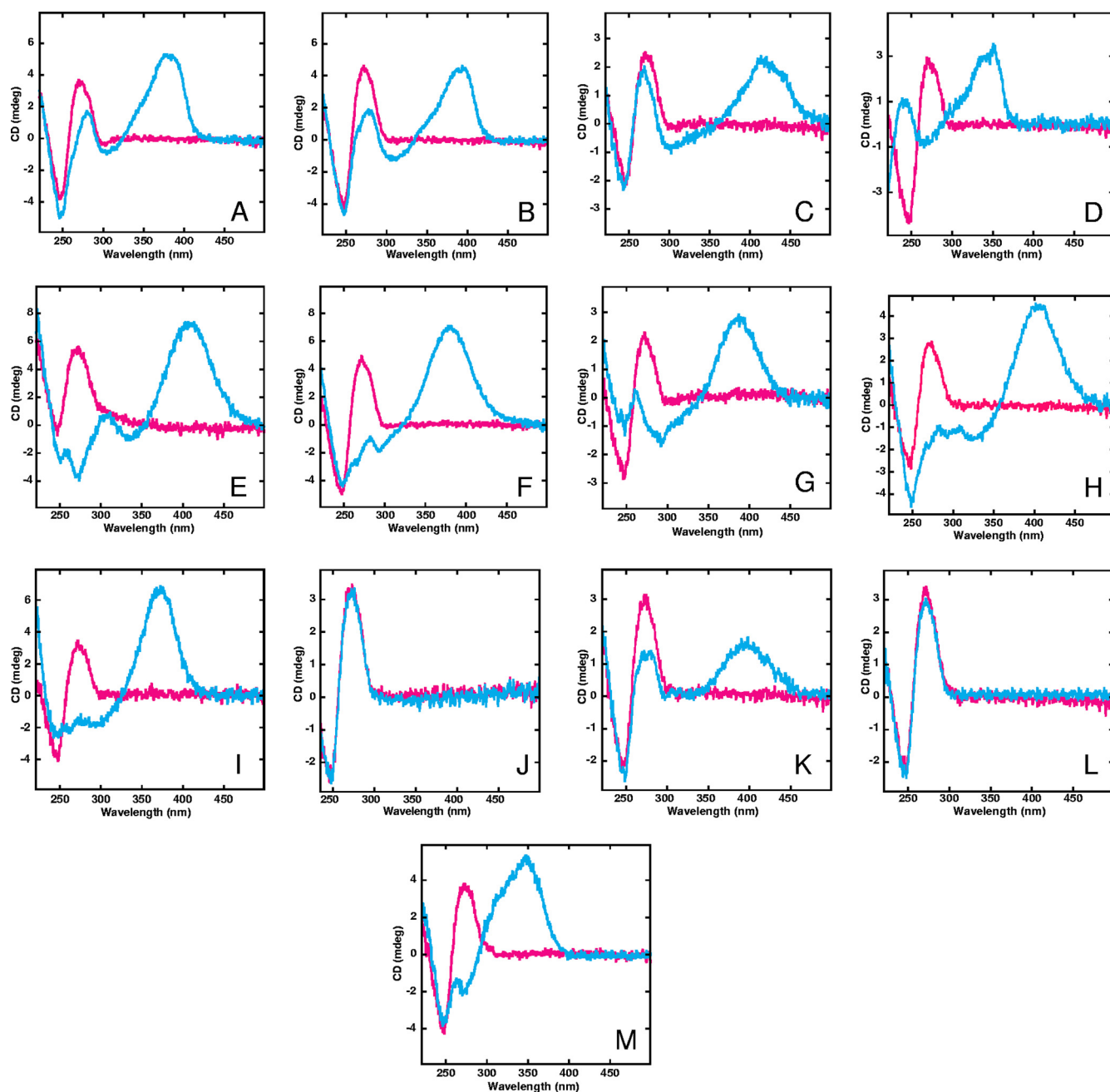


FIG. 3. (A to M) CD spectra of amidines incubated with purified kDNA network of epimastigotes of *T. cruzi* using a compound-to-kDNA base pair ratio of 0.2. A spectrum for DNA without compound is shown in red and has no induced signal. (A) DB75; (B) DB569; (C) DB1345; (D) DB829; (E) DB766; (F) DB749; (G) DB889; (H) DB709; (I) DB613; (J) DB1831; (K) DB1852; (L) DB2002; and (M) DB1080.

Interestingly, the two AIAs (DB1831 and DB2002) that did not bind to the conserved minicircle sequence (Table 2 and Fig. 1F and H) also did not associate with the whole kDNA when CD (Fig. 3J and L) or T_m assays (Table 2) were employed.

DISCUSSION

Using peculiar characteristics of trypanosomatid parasites as targets is a fundamental approach for the design of novel and

selective drugs (37). Regarding ADs, which bind strongly to AT sequences of four or more base pairs, one of those proposed interaction targets is the unique DNA present in the mitochondria of trypanosomatids, the kDNA, although others, such as the RNA, also have been proposed (40). For this reason, the anti-*T. cruzi* effect of 13 structurally related amidines was evaluated, and their kDNA binding affinities were determined through CD and T_m studies aiming to verify whether they could bind to the kDNA, inducing changes in its structure and what correlations exist for affinity, structural changes, and activity.

Regarding the biological data, epimastigotes were less susceptible to the compounds than to BT, which corroborates previous data obtained with ADs (3). Interestingly, DB829 had very low activity against epimastigotes (IC₅₀ of 938 mM) and trypomastigotes (IC₅₀ of 437 mM) of *T. cruzi*, although it has been effective against *T. brucei* subsp. *rhodesiense* (18.7 nM) (17). This difference in susceptibility among *T. brucei* and *T. cruzi* as well as between different parasite forms within the same specie (*T. cruzi*) likely involves a (i) dissimilar mechanisms of action and/or (ii) differences in compound uptake by these parasites. Other explanations could include the existence of distinct cellular targets, different kDNA organization, different kinetics for the compound distribution and accumulation, and/or distinct modes of drug extrusion. Another interesting finding is that the biological activity against epimastigotes confirmed previous results in *Leishmania major*, *Leishmania tropica* (31), BT, and intracellular forms of *T. cruzi* (3, 33, 34, 39) that showed a greater effect of AIAs than other classical amidines. The reverse situation holds for *T. brucei*, suggesting that there are significant differences in mechanisms of action of amidines among these organisms.

To determine whether these amidines target sequences in kinetoplast DNA, thermodynamic studies were performed using not only synthetic conserved minicircle sequences but also whole purified kDNA networks of *T. cruzi*, since these native networks may lead to more objective and precise results than synthetic homopolymers. Additionally, although there is no experimental evidence of a functional role for the minicircle sequence presently chosen, it comprises a conserved sequence (AGG GGC GTT C) present in different trypanosomes and overlaps the 5' termini of newly synthesized minicircles of *C. fasciculata*, suggesting a potential role in replication initiation (30). Additionally, compound association to any other sequences in the whole kDNA could interfere in essential processes, such as parasite replication, transcription, and/or the RNA editing process (1, 42).

CD and ΔT_m analysis confirmed previous studies that demonstrated the strong DNA binding characteristics of DB75 (20). This AD strongly bound the minicircle synthetic sequence (ΔT_m of 17°C and positive induced CD) and the whole *T. cruzi* kDNA (ΔT_m of 15°C and positive induced CD), although not as strongly as previously observed for the polymer AT sequence (ΔT_m of 26°C) (21). Clearly, sequences other than those with AT base pairs are affecting the compound-kDNA interaction with the minicircle conserved sequence as well as in the whole kDNA.

Also, no correlation was found between kDNA T_m increase and trypanocidal activity in *T. cruzi*: despite its high biological activity, DB1831 and DB766 do not bind to the purified whole kDNA (ΔT_m of 0°C), while some of the compounds that had the lowest activity, such as DB75, DB1345, DB829, and DB1080, showed the highest relative binding values. Another example is DB75 and DB569, which presented similar affinity for the whole purified parasite kDNA; however, the N-phenyl-substituted compound is approximately 100 times more active than DB75. These data demonstrate that the mechanism of action of amidines on trypanosomatids may not be universal and cannot be attributed only to the binding affinities to the parasite kDNA, and thus other cellular targets may also be involved. Recent published data from our group showed that, similarly to observations with *T. brucei*, diamidines also are

accumulated within DNA-free organelles, possibly acidocalcisomes (3), which are acidic organelles that play roles in a number of cellular processes, such as the storage of cations and phosphorus, calcium homeostasis, the maintenance of intracellular pH, and osmoregulation (14). Additionally, although diamidines are localized within the nuclei and kDNA of *T. cruzi*, their higher accumulation in the latter structure does not predict compound efficacy *in vitro* (5, 8).

Concerning the chemical structures, we showed that small changes, such as nitrogen atom addition, result in large differences in their ability to bind to the kDNA, as reported previously (44). This is readily observed for DB766 and DB1831, which differ by one nitrogen atom in each of the terminal rings (Fig. 1) but display different capabilities to induce positive CDs.

In summary, our T_m data suggest that the affinity of amidines for kDNA is not sufficient to generate and trigger their trypanocidal activity, and that other mechanisms of action are operating in the parasite death. In fact, our CD studies demonstrated that although they are not strong kDNA binders, some highly effective AIAs, like DB766, are able to profoundly alter the parasite kDNA topology, suggesting that specific topological effects are more relevant to the biological activity of amidines than the simple binding affinity characteristics. These topological alterations at the kDNA may contribute to parasite death by impairing the access and perfect connection of enzymes as well as other important molecules involved in essential cellular processes. Further molecular and biochemical studies are under way to better understand the mechanisms of action of this class of compounds which may contribute to the search for novel and selective drugs for parasitic disease treatment.

ACKNOWLEDGMENTS

The present study was supported by grants from Fundação Carlos Chagas Filho de Amparo a Pesquisa do Estado do Rio de Janeiro (FAPERJ/APO); Rede de Plataformas PDTIS/VPPLR/Fiocruz; Apoio ao Desenvolvimento Científico e Tecnológico Regional do Rio de Janeiro (2011); Pronex-Faperj (17/2009), Pensa-Rio (16/2009-E-26/110-313/2010), Conselho Nacional de Desenvolvimento Científico e Tecnológico (CNPq), PAPES V/FIOCRUZ, Coordenação de Aperfeiçoamento Pessoal do Ensino Superior (CAPES); Consortium for Parasitic Drug Development (CPPD); and National Institutes of Health grant AI064200 (to W.D.W. and D.W.B.).

We are also grateful to Hiu Zhao from the Core Facility of Georgia State University for the technical support with the atomic force microscopy analyses.

REFERENCES

- Amaro, R. E., et al. 2008. Discovery of drug-like inhibitors of an essential RNA-editing ligase in *Trypanosoma brucei*. Proc. Natl. Acad. Sci. U. S. A. **105**:17278–17283.
- Arafa, R. K., et al. 2005. Synthesis, DNA affinity, and antiprotozoal activity of fused ring dicationic compounds and their prodrugs. J. Med. Chem. **48**:5480–5488.
- Batista, D. G., et al. 2010. Arylimidamide DB766, a potential chemotherapeutic candidate for Chagas' disease treatment. Antimicrob. Agents Chemother. **54**:2940–2952.
- Camargo, E. P. 1964. Growth and differentiation in *Trypanosoma cruzi*. I. Origin of metacyclic trypanosomes in liquid media. Rev. Inst. Med. Trop. São Paulo **6**:93–100.
- Daliry, A., et al. 2009. *In vitro* analyses of the effect of aromatic diamidines upon *Trypanosoma cruzi*. J. Antimicrob. Chemother. **64**:747–750.
- Das, B. P., and D. W. Boykin. 1977. Synthesis and antiprotozoal activity of 2,5-bis-(4-guanidylphenyl) furans. J. Med. Chem. **20**:531–536.
- da Silva, C. F., et al. 2008. Trypanocidal activity of a diarylthiophene diamidine against *Trypanosoma cruzi*: *in vitro* and *in vivo* studies. Antimicrob. Agents Chemother. **52**:3307–3314.

8. **da Silva, C. F., et al.** 2010. The biological *in vitro* effect and selectivity of aromatic dicationic compounds on *Trypanosoma cruzi*. Mem. Inst. Oswaldo Cruz **105**:239–245.
9. **De Souza, E. M., et al.** 2004. Phenyl substitution of furamidine markedly potentiates its antiparasitic activity against *Trypanosoma cruzi* and *Leishmania amazonensis*. Biochem. Pharmacol. **68**:593–600.
10. **De Souza, E. M., et al.** 2006. Trypanocidal activity of the phenyl-substituted analogue of furamidine DB569 against *Trypanosoma cruzi* infection *in vivo*. J. Antimicrob. Chemother. **58**:610–614.
11. **De Souza, E. M., et al.** 2011. Trypanocidal activity and selectivity *in vitro* of aromatic amidine compounds upon bloodstream and intracellular forms of *Trypanosoma cruzi*. Exp. Parasitol. **127**:429–435.
12. **Degrave, W., et al.** 1988. Peculiar sequence organization of kinetoplast DNA minicircles from *Trypanosoma cruzi*. Mol. Biochem. Parasitol. **27**:63–70.
13. **de Meirelles, M. N., T. C. Araújo-Jorge, and W. de Souza.** 1982. Interaction of *Trypanosoma cruzi* with macrophages *in vitro*: dissociation of the attachment and internalization phases by low temperature and cytochalasin B. Z. Parasitenkd. **68**:7–14.
14. **Docampo, R., P. Ulrich, and S. N. Moreno.** 2010. Evolution of dicolocalisomes and their role in polyphosphate storage and osmoregulation in eukaryotic microbes. Philos. Trans. R. Soc. Lond. B Biol. Sci. **365**:775–784.
15. **Estévez, A. M., and L. Simpson.** 1999. Uridine insertion/deletion RNA editing in trypanosome mitochondria—a review. Gene **240**:247–260.
16. **González, A.** 1986. Nucleotide sequence of a *Trypanosoma cruzi* minicircle. Nucleic Acids Res. **14**:9217.
17. **Ismail, M. A., et al.** 2003. Synthesis and antiprotozoal activity of aza-analogues of furamidine. J. Med. Chem. **46**:4761–4769.
18. **Lanteri, C. A., R. R. Tidwell, and S. R. Meshnick.** 2008. The mitochondrion is a site of trypanocidal action of the aromatic diamidine DB75 in bloodstream forms of *Trypanosoma brucei*. Antimicrob. Agents Chemother. **52**:875–882.
19. **Liu, B., Y. Liu, S. A. Motyka, E. E. Agbo, and P. T. P. T. Englund.** 2005. Fellowship of the rings: the replication of kinetoplast DNA. Trends Parasitol. **21**:363–369.
20. **Liu, Y., A. Kumar, D. W. Boykin, and W. D. Wilson.** 2007. Sequence and length dependent thermodynamic differences in heterocyclic diamidine interactions at AT base pairs in the DNA minor groove. Biophys. Chem. **131**:1–14.
21. **Mathis, A. M., et al.** 2007. Diphenyl furans and Aza analogs: effects of structural modification on *in vitro* activity, DNA binding, and accumulation and distribution in trypanosomes. Antimicrob. Agents Chemother. **51**:2801–2810.
22. **Mdachi, R. E., et al.** 2009. Efficacy of the novel diamidine compound 2,5-bis(4-amidinophenyl)-furan-bis-O-methylamidoxime (pafuramidine, DB289) against *Trypanosoma brucei rhodesiense* infection in vervet monkeys after oral administration. Antimicrob. Agents Chemother. **53**:953–957.
23. **Morel, C., et al.** 1980. Strains and clones of *Trypanosoma cruzi* can be characterized by pattern of restriction endonuclease products of Kinetoplast DNA minicircles. Proc. Natl. Acad. Sci. U. S. A. **77**:6810–6814.
24. **Moreno, S. N.** 1996. Pentamidine is an uncoupler of oxidative phosphorylation in rat liver mitochondria. Arch. Biochem. Biophys. **326**:15–20.
25. **Onn, I., I. Kapeller, K. Abu-Elneel, and J. Shlomai.** 2006. Binding of the universal minicircle sequence binding protein at the kinetoplast DNA replication origin. J. Biol. Chem. **281**:37468–37476.
26. **Pacheco, M. G., et al.** 2009. *Trypanosoma cruzi*: activity of heterocyclic cationic molecules *in vitro*. Exp. Parasitol. **123**:73–80.
27. **Pacheco, R. S., Jr., G. Grimaldi, H. Momen, and C. M. Morel.** 1990. Populational heterogeneity among clones of New World *Leishmania* species. Parasitology **100**:393–398.
28. **Pacheco, R. S., et al.** 1998. Chagas' disease and HIV co-infection: genotypic characterization of the *Trypanosoma cruzi* strain. Mem. Inst. Oswaldo Cruz **93**:165–169.
29. **Ray, D. S.** 1987. Kinetoplast DNA minicircles: high-copy-number mitochondrial plasmids. Plasmid **17**:177–190.
30. **Ray, D. S.** 1989. Conserved sequence blocks in kinetoplast minicircles from diverse species of trypanosomes. Mol. Cell. Biol. **9**:1365–1367.
31. **Rosypal, A. C., et al.** 2008. Inhibition by dicationic *in vitro* growth of *Leishmania major* and *Leishmania tropica*: causative agents of old world cutaneous leishmaniasis. J. Parasitol. **94**:743–749.
32. **Shapiro, T. A., and P. T. Englund.** 1995. The structure and replication of kinetoplast DNA. Annu. Rev. Microbiol. **49**:117–143.
33. **Silva, C. F., et al.** 2007. Cellular effects of reversed amidines on *Trypanosoma cruzi*. Antimicrob. Agents Chemother. **51**:3803–3809.
34. **Silva, C. F., et al.** 2007. Activity of “reversed” diamidines against *Trypanosoma cruzi in vitro*. Biochem. Pharmacol. **73**:1939–1946.
35. **Simpson, L., and J. Berliner.** 1974. Isolation of the kinetoplast DNA of *Leishmania tarentolae* in the form of a network. J. Protozool. **21**:382–393.
36. **Simpson, L., R. Aphasizhev, G. Gao, and X. Kang.** 2004. Mitochondrial proteins and complexes in *Leishmania* and *Trypanosoma* involved in U-insertion/deletion RNA editing. RNA **10**:159–170.
37. **Soeiro, M. N. C., and S. L. de Castro.** 2009. *Trypanosoma cruzi* targets for new chemotherapeutic approaches. Expert Opin. Ther. Targets. **13**:105–121.
38. **Stephens, C. E., et al.** 2001. Diguandino and “reversed” diamidino 2,5-diarylfurans as antimicrobial agents. J. Med. Chem. **44**:1741–1748.
39. **Stephens, C. E., et al.** 2003. The activity of diguanidino and “reversed” diamidino 2,5-diarylfurans versus *Trypanosoma cruzi* and *Leishmania donovani*. Bioorg. Med. Chem. Lett. **13**:2065–2069.
40. **Sun, T., and Y. Zhang.** 2008. Pentamidine binds to tRNA through non-specific hydrophobic interactions and inhibits aminoacylation and translation. Nucleic Acids Res. **36**:1654–1664.
41. **Urbina, J. A.** 2010. Specific chemotherapy of Chagas disease: relevance, current limitations and new approaches. Acta Trop. **115**:55–68.
42. **Wang, B., et al.** 2003. TbMP44 is essential for RNA editing and structural integrity of the editosome in *Trypanosoma brucei*. Eukaryot. Cell **2**:578–587.
43. **Wang, M. Z., et al.** 2010. Novel arylimidamides for the treatment of visceral leishmaniasis. Antimicrob. Agents Chemother. **54**:2507–2516.
44. **Wilson, W. D., et al.** 2008. Antiparasitic compounds that target DNA. Biochimie **90**:999–1014.